Published in final edited form as:
Dev Biol. 2019 May 15; 449(2): 90–98. doi:10.1016/j.ydbio.2019.02.017.

Myosin heavy chain mutations that cause Freeman-Sheldon syndrome lead to muscle structural and functional defects in *Drosophila*

Shreyasi Das[a], **Pankaj Kumar**[a,c], **Aakanksha Verma**[a], **Tushar K. Maiti**[b], **Sam J. Mathew**[a,c,*]

[a]Laboratory of Developmental Genetics, Regional Centre for Biotechnology, NCR Biotech Science Cluster, 3rd Milestone, Faridabad-Gurgaon Expressway, Faridabad, Haryana, 121001, India

[b]Functional Proteomics Laboratory, Regional Centre for Biotechnology, NCR Biotech Science Cluster, 3rd Milestone, Faridabad-Gurgaon Expressway, Faridabad, Haryana, 121001, India

[c]Affiliated to Manipal Academy of Higher Education, Manipal, Karnataka, 576104, India

Abstract

Missense mutations in the *MYH3* gene encoding myosin heavy chain-embryonic (MyHC-embryonic) have been reported to cause two skeletal muscle contracture syndromes, Freeman Sheldon Syndrome (FSS) and Sheldon Hall Syndrome (SHS). Two residues in MyHC-embryonic that are most frequently mutated, leading to FSS, R672 and T178, are evolutionarily conserved across myosin heavy chains in vertebrates and *Drosophila*. We generated transgenic *Drosophila* expressing myosin heavy chain (*Mhc*) transgenes with the FSS mutations and characterized the effect of their expression on *Drosophila* muscle structure and function. Our results indicate that expressing these mutant *Mhc* transgenes lead to structural abnormalities in the muscle, which increase in severity with age and muscle use. We find that flies expressing the FSS mutant *Mhc* transgenes in the muscle exhibit shortening of the inter-Z disc distance of sarcomeres, reduction in the Z-disc width, aberrant deposition of Z-disc proteins, and muscle fiber splitting. The ATPase activity of the three FSS mutant MHC proteins are reduced compared to wild type MHC, with the most severe reduction observed in the T178I mutation. Structurally, the FSS mutations occur close to the ATP binding pocket, disrupting the ATPase activity of the protein. Functionally, expression of the FSS mutant *Mhc* transgenes in muscle lead to significantly reduced climbing capability in adult flies. Thus, our findings indicate that the FSS contracture syndrome mutations lead to muscle

*Corresponding author. Laboratory of Developmental Genetics, Regional Centre for Biotechnology, NCR Biotech Science Cluster, 3rd Milestone, Faridabad-Gurgaon Expressway, Faridabad, Haryana, 121001, India. sjmathew@rcb.res.in (S.J. Mathew).

Conflicts of interest

The authors declare no competing or financial interests.

Author contributions statement

SJM and SD conceived the project and designed the experiments. The experiments were carried out by SD with support from PK and AV, under the guidance of SJM. TKM did the MHC structural modeling. The data was analyzed and figures compiled by PK, SD, TKM, and SJM. The manuscript was written by SJM with inputs from SD and TKM. All authors have read and approve the manuscript. Funding for this work was secured by SJM.

Note

Rao et al (Mol Biol Cell 2019; 30(1):30–41) published work on FSS mutations in *Drosophila* while this manuscript was in revision.

structural defects and functional deficits in *Drosophila*, possibly mediated by the reduced ATPase activity of the mutant MHC proteins.

Keywords

Skeletal muscle; Myosin heavy chain; Freeman-Sheldon syndrome; Contracture; Sarcomere; Drosophila

Europe PMC Funders Author Manuscripts

1 Introduction

Myosins are motor proteins that are essential for a wide array of fundamental cellular functions such as motility, division, and transport. In the skeletal and cardiac muscle, specialized myosins belonging to the class II myosin family are involved in facilitating muscle contraction (Sellers, 2000). The skeletal muscle myosins are heterohexamers, comprising a pair of myosin heavy chains (MyHCs), a pair of essential light chains and a pair of regulatory light chains (Schiaffino and Reggiani, 1996). MyHCs possess ATPase activity and interact with actin, properties that are critical for muscle contraction. Mammals have multiple MyHC isoforms with distinct ATPase activity, and their distribution in muscle fibers is thought to be determined by the anatomical location and functional output of the muscle (Schiaffino and Reggiani, 1996).

Two MyHC isoforms are expressed primarily during mammalian development, of which mutations in one of them, *MYH3* which codes for MyHC-embryonic protein, have been reported to lead to Freeman-Sheldon (FSS) or Sheldon-Hall (SHS) contracture syndromes (Tajsharghi et al., 2008; Toydemir et al., 2006). Patients with FSS or SHS typically exhibit contractures of the orofacial muscles, camptodactyly, clubfeet and scoliosis (Tajsharghi et al., 2008; Toydemir et al., 2006). SHS occurs more frequently compared to FSS, with the severity of the facial contractures relatively less in SHS (Beck et al., 2014; Toydemir et al., 2006). Missense mutations in *MYH3* and other muscle contractile genes can cause FSS and SHS, although the most frequently mutated gene leading to these syndromes is *MYH3* (Bamshad et al., 2009). Though the gene which is mutated in the majority of FSS and SHS cases has been identified, no animal models to study these syndromes have been reported. Mouse models for FSS or SHS are a possibility, but the presence of additional MyHC isoforms that could compensate for MyHC-embryonic could complicate interpretations from such studies (Sharma et al., 2018).

Here, we used *Drosophila* as a model to gain insights into the MyHC mutations that cause FSS. *Drosophila* has a single muscle myosin heavy chain gene (*Mhc*), and therefore, compensation by other MyHC isoforms will not confound results. In addition, the muscle architecture in *Drosophila* has significant similarities to that of vertebrates, with several structural and contractile proteins conserved evolutionarily (Rui et al., 2010).

We find that the residues in MyHC-embryonic that are most frequently mutated, leading to FSS are conserved evolutionarily across vertebrates and in *Drosophila*. By expressing *Mhc* transgenes that carry the FSS mutations in *Drosophila* muscle, we have generated a model to study these contracture syndromes. Our results indicate that expressing these mutant *Mhc*

transgenes lead to muscle structural abnormalities, which increase in severity with age and muscle use. We find that the inter-Z disc length of sarcomeres is significantly shortened, the Z-disc width is reduced, Z-disc proteins are aberrantly deposited, and extensive muscle fiber splitting occurs upon expressing the *Mhc* transgenes in the *Drosophila* muscle. We also find that the ATPase activity of the FSS mutant MHC proteins are reduced compared to wild type MHC. Analyzing the protein structure, we find that the FSS mutant residues lie close to the ATP binding pocket of MHC and therefore disrupt its catalytic activity. Functionally, expression of the mutant *Mhc* transgenes lead to reduced climbing capability in adult flies. Thus, our findings indicate that the FSS contracture syndrome mutations lead to muscle structural defects and functional deficits in *Drosophila*. Since such severe effects on sarcomeric organization have so far not been reported from human patients with FSS, we hypothesize that the presence of multiple MyHC isoforms compensates for mutated MyHC-embryonic in humans with these syndromes. Our results also suggest that the decreased ATPase activity, sarcomere defects and functional deficits that we observe in flies expressing the FSS mutant *Mhc* transgenes are interlinked.

2 Results

2.1 MYH3 residues most frequently mutated in FSS are evolutionarily conserved

The most frequent mutations in MyHC-embryonic that cause Freeman-Sheldon syndrome (FSS) are R672H, R672C and T178I (Beck et al., 2014; Toydemir et al., 2006). T178I has been reported to lead to the relatively less severe Sheldon-Hall syndrome (SHS) also, although later those individuals were reclassified based on phenotype as FSS patients (Beck et al., 2014; Toydemir et al., 2006). Both R672 and T178 residues are in the head domain of the MyHC, critical for ATPase activity and actin binding, essential for contractile function of the myosin motor (Fig. 1A). We found that R672 and T178 are highly conserved evolutionarily, across vertebrates and in *Drosophila* muscle myosin heavy chain (MHC) (Fig. 1B and C). Interestingly, the neighboring residues, that form part of the hydrophobic core region of MHC are also evolutionarily conserved, indicating that they might be part of sub-domains that have crucial roles in myosin function (Fig. 1B and C). Comparing the human MyHC-embryonic and *Drosophila* MHC across their entire sequence, we found that they are ~55% similar (data not shown).

The crystal structure of *Drosophila* MHC (available from PDB: PDB ID 5W1A) reveals that Threonine 178 and Arginine 672 residues are closely packed within the hydrophobic core constituted mainly by four Phenylalanine residues (F122, F487, F488 and F470), Leucine 176, Leucine 689, Valine 124 and Valine 699 (Fig. 1D, D′). The side chain of Arginine (R672) is nicely packed within the hydrophobic pocket created by several phenylalanine residues. The positive charge of the R672 side chain amine group is stabilized by π-charge interaction (Dougherty, 1996; Walklate et al., 2016; Wheeler and Bloom, 2014). While the R672C mutation disrupts the π-charge interaction, in R672H, incorporation of large histidinium ion may push the well aligned hydrophobic residues, rendering the pocket unstable. Both loss of π-charge interaction as well as loss of hydrophobic packing may thus affect activity in R672C and R672H mutations respectively. Similarly, the T178I mutation breaks the polar interaction between R672 and T178 residues (Walklate et al., 2016). A

previous study where the R672C, R672H and T178I mutant human MyHC-embryonic proteins were expressed using a recombinant system found that all three mutations affected the kinetics, especially the ATP hydrolysis properties of the protein (Walklate et al., 2016).

2.2 Expression of FSS mutant *Mhc* transgenes in *Drosophila* lead to sarcomeric defects

To test the role of the T178 and R672 residues in MHC function in *Drosophila*, we generated four transgenic fly stocks, each with wild type *Drosophila Mhc*, or *T178I*, *R672C* and *R672H* mutations in *Drosophila Mhc* (Mhc^{wt}, Mhc^{T178I}, Mhc^{R672C} and Mhc^{R672H} respectively), under the control of an Upstream Activating Sequence (UAS). To study the effect of expressing these transgenes in the *Drosophila* muscle, we brought them in the Mhc^{1} mutant background, which is a null mutation for the *Drosophila Mhc* gene (O'Donnell and Bernstein, 1988). We used the *Mef2GAL4* driver line to express the *Mhc* transgenes in the muscle (Gunage et al., 2014; Schnorrer et al., 2010). Mhc^{1} heterozygous mutant flies exhibit muscle defects and we performed our experiments in this background, since Mhc^{1} homozygous mutants die as embryos (O'Donnell and Bernstein, 1988). These transgenic stocks in the Mhc^{1} heterozygous background with *Mef2Gal4* driving their expression are designated *Mhc* (wild type *Mhc* transgene), *R672H* (*R672H* mutant transgene), *R672C* (*R672C* mutant transgene) and *T178I* (*T178I* mutant transgene) respectively. The actual genotypes of each of these stocks when analyzed are Mhc^{1}/CyO; *Mef2GAL4/UAS-*Mhc^{wt}, Mhc^{1}/CyO; *Mef2GAL4/UAS-*Mhc^{R672H}, Mhc^{1}/CyO; *Mef2GAL4/UAS-*Mhc^{R672C} *and* Mhc^{1}/CyO; *Mef2GAL4/UAS-*Mhc^{T178I}.

In the Mhc^{1} heterozygous background, we found that expressing the wild type *Mhc* transgene led to relatively normal muscle fibers and Z-discs marked by Kettin in the adult dorsal longitudinal muscles (DLMs) compared to the DLMs of wild type *Canton S* flies, within 5 days of eclosion (compare Fig. 2E-H with A-D). Since the wild type *Mhc* transgene is inserted at the same locus and is in the same background as the mutant *Mhc* transgenes, to control for the effect of overexpression, all statistical comparisons of the FSS mutant *Mhc* transgenes were made with flies expressing the wild type *Mhc* transgene. There were minor defects in Z-disc material deposition and fiber splitting in the DLMs of flies expressing the wild type *Mhc* transgene. However, flies expressing the FSS mutations – *R672H*, *R672C* and *T178I* exhibited severe fiber branching and splitting defects (Fig. 2I-L, M-P and Q-T and Fig. 5). We observed the most severe defects in flies expressing the *R672C* transgene where the Z-disc material marked by Kettin protein was not uniformly deposited and was fragmented (Arrowheads in Fig. 2P).

Next, we tested whether muscle use has any effect on the DLMs expressing the *Mhc* transgenes. Therefore, we performed immunofluorescence to label the sarcomeres of DLMs from 3-week-old *Canton S*, wild type *Mhc* transgenic and FSS mutant *Mhc* transgenic flies in the Mhc^{1} heterozygous background. Interestingly, we found that the branching phenotype observed at 5 days post-eclosion persisted at 3 weeks of age in wild type *Mhc* expressing flies compared to *Canton S* (Fig. 5). Similarly, flies expressing the FSS mutations – *R672H*, *R672C* and *T178I* continued to exhibit severe fiber branching defects (Fig. 3I-L, M-P and Q-T and Fig. 5). The Z-disc material marked by Kettin protein appeared abnormal, absent in some regions and most severe in DLMs from flies expressing the *R672C* and *R672H*

transgenes (Fig. 3L and P). We did not find significant overexpression effects when the *Mhc*^{wt} construct was expressed in the wild type background, at 5 or 20 days post-eclosion, indicating that the observed effects occur specifically in the *Mhc*^{1} heterozygous background (Supplementary Fig. 2).

We quantified the sarcomeric defects observed in the DLMs at 5 days and 20 days post-eclosion. For this, we quantified the inter-Z disc distance which is a measure of the length of the sarcomere, and the Z-disc width which is a measure of the width of the sarcomere (Fig. 4A). The Kettin staining of DLMs from *Canton S*, and the different *Mhc* transgenic flies in the *Mhc*^{1} background were used for this quantification. We found that DLMs from all three FSS mutant - *R672H*, *R672C* and *T178I* exhibited significant shortening of the inter-Z disc distance at 5 days post-eclosion, compared to wild type flies (Fig. 4B). Confirming the qualitative observation, *R672C* expressing flies exhibited the most severe shortening of the sarcomere to almost half as that of a wild type sarcomere (Fig. 4B). The Z-disc width was significantly reduced in *R672H* and *R672C* flies at 5 days post-eclosion (Fig. 4C).

At 20 days post-eclosion, the inter-Z disc distance continued to be significantly reduced in all three FSS mutants (Fig. 4D). While the severe effect on *R672C* improved marginally, *R672H* exhibited a similar level of inter-Z disc distance shortening as *R672C* by 20 days, indicating that muscle use could lead to distinct outcomes in the different mutations. Interestingly, the Z-disc width was significantly reduced in all three FSS mutant lines by 20 days, indicating that muscle use or aging leads to shortening of the sarcomeric width in these *Mhc* mutants (Fig. 4E).

Comparing the inter-Z disc distance and the Z-disc width for flies of the same genotype between 5 and 20 days post-eclosion, we found that the inter-Z disc distance decreased significantly with age in *R672H* and *T178I* expressing flies, while it increased significantly in *R672C* expressing flies (Fig. 4F). The increase observed in *R672C* could be because the inter-Z disc distance is shortest in *R672C* expressing flies at 5 days post-eclosion (Fig. 4B). The Z-disc width changed significantly only in the *T178I* expressing flies with age, where it decreased significantly by 20 days post-eclosion (Fig. 4G). Thus, it seems that inter-Z disc distance is a sarcomeric attribute more likely to change with age or muscle use than Z-disc width.

We also quantified the degree of fiber splitting by counting the number of split fibers as a proportion of total fibers in the different *Mhc* transgenic flies in the *Mhc*^{1} background (Fig. 5). At 5 days post-eclosion, about 20% of fibers were split in *Mhc*^{wt} expressing flies (Fig. 5B, B′ and K). In comparison, the FSS mutant *Mhc* expressing flies exhibited a statistically significant increase in split fibers, with R672H and T178I expressing flies exhibiting ~40% and R672C expressing flies ~70% split fibers (Fig. 5A-E′, K). At 20 days post-eclosion, we observed that ~40% fibers were split in the *Mhc*^{wt} expressing flies, suggesting that muscle use and age leads to increased fiber splitting (Fig. 5G, G′ and L). We also found that all FSS mutant *Mhc* expressing flies exhibited ~80% or more split fibers at 20 days post-eclosion, a statistically significant effect compared to *Mhc*^{wt} expressing flies (Fig. 5F-J′, L). Thus, expressing the FSS mutant transgenes led to increased fiber splitting compared to controls at

5 days post-eclosion, which exacerbated further with muscle use and age by 20 days post-eclosion.

2.3 FSS mutant *Mhc* transgenes exhibit reduced ATPase activity

We next tested the ATPase activity of the FSS mutant MHC proteins expressed in flies compared to wild type MHC. We isolated the DLMs from about 50 flies each of *Canton S*, *Mhc^{1}/CyO; Mef2GAL4/UAS-Mhc^{wt}*, *Mhc^{1}/CyO; Mef2GAL4/UAS-Mhc^{R672H}*, *Mhc^{1}/CyO; Mef2GAL4/UAS-Mhc^{R672C} and Mhc^{1}/CyO; Mef2GAL4/UAS-Mhc^{T178I}* genotypes. MHC from each of the genotypes was extracted, quantified and separated on SDS PAGE to ensure proper extraction and enrichment of MHC (Fig. 6A). ATPase assay for MHC was carried out using mouse skeletal muscle Actin, based on the change in absorbance at 360 nm of 2-amino-6-marcapto-7-methyl-purine riboside (MESG) by purine nucleoside phosphorylase (PNP) (Webb, 1992). We found that compared to *Canton S* MHC protein, overexpressed MHC^{wt} had comparable ATPase activity. MHC^{R672H} exhibited slightly reduced ATPase activity, MHC^{R672C} even lesser and MHC^{T178I} had the least activity among the FSS mutant MHCs (Fig. 6B). Thus, all 3 FSS mutant MHC proteins exhibited reduced ATPase activity compared to wild type MHC, as reported previously (Walklate et al., 2016).

2.4 Expression of FSS mutant *Mhc* transgenes in *Drosophila* lead to functional defects

Since we observed sarcomeric structural defects upon expressing the FSS mutant *Mhc* transgenes and aberrant ATPase activity for the mutant MHC proteins, we tested whether these translated to functional defects in flies. Muscle activity is required for eclosion of adult flies from their pupal case (Hatfield et al., 2015). Therefore, we compared the pupal duration of flies overexpressing the *Mhc* transgenes in the *Mhc^{1}* heterozygous background with *Mef2GAL4* driving their expression (*Mhc^{1}/CyO; Mef2GAL4/UAS-Mhc^{wt}*, *Mhc^{1}/CyO; Mef2GAL4/UAS-Mhc^{R672H}*, *Mhc^{1}/CyO; Mef2GAL4/UAS-Mhc^{R672C} and Mhc^{1}/CyO; Mef2GA-L4/UAS-Mhc^{T178I}*). We observed that compared to wild type *Canton S* flies, all of the *Mhc* transgene overexpressing flies spent a significantly longer duration as pupae (Fig. 7A). Compared to *Mhc^{wt}* expressing flies, *Mhc^{R672H}*, and *Mhc^{T178I}* expressing flies exhibited a trend towards increased pupal duration, although this effect was not statistically significant (Fig. 7A).

We also carried out climbing assays to test muscle function and found that at 5 days post-eclosion, *Mhc^{1}/CyO; Mef2GAL4/UAS-Mhc^{R672H}* and *Mhc^{1}/CyO; Mef2GAL4/UAS-Mhc^{R672C}* flies exhibited significantly reduced climbing capability compared to *Mhc^{1}/CyO; Mef2GAL4/UAS-Mhc^{wt}* flies (Fig. 7B). By 20 days post-eclosion, all 3 FSS mutants (*Mhc^{1}/CyO; Mef2GAL4/UAS-Mhc^{R672H}*, *Mhc^{1}/CyO; Mef2GAL4/UAS-Mhc^{R672C} and Mhc^{1}/CyO; Mef2GAL4/UAS-Mhc^{T178I}*) exhibited significantly diminished climbing capability compared to *Mhc^{1}/CyO; Mef2GAL4/UAS-Mhc^{wt}* flies (Fig. 7C). This indicates that muscle function is significantly compromised in the FSS mutant *Mhc* overexpressing flies, and this effect aggravates with muscle use and age.

3 Discussion

The MyHC-embryonic isoform in mammals is thought to be predominantly expressed during developmental stages and is only expressed in adults during muscle injury or disease (Sharma et al., 2018). It is not well understood how mutations in MyHC-embryonic lead to FSS and SHS (Sharma et al., 2018). In this paper, we have expressed FSS mutant myosin heavy chain in *Drosophila* muscle to decipher the effect of those mutations on muscle structure and function. We find that the FSS mutant myosins cause muscle structural abnormalities, especially shortening of the sarcomeric length and width, and myofiber branching, phenotypes which become more pronounced with muscle use and age. The sarcomere shortening phenotype that we observe could underlie the contractures observed in FSS patients. Some studies where morphologic analysis of muscle samples was carried out reports increased fiber size variability due to predominance of small, type I fibers in FSS patients (Kimber et al., 2012; Tajsharghi et al., 2008). Similar to our observations with MHC and the thick filament in this work, previous reports indicate that thin filament assembly defects lead to shortened sarcomeres in *Drosophila* muscle (Bai et al., 2007).

By using *Drosophila* as model, where there is a single muscle *Mhc* gene, we have overcome the compensatory effects by other myosin heavy chain isoforms, which could alleviate the phenotype in human FSS and SHS patients (Tajsharghi et al., 2008). Since we observe sarcomere shortening in *Drosophila* expressing the mutant MHC, it is possible that the effect of the FSS mutations occurs during early embryonic development, where only MyHC-embryonic and MyHC-slow are expressed and other MyHC isoforms may not be able to compensate since they are not expressed at those stages (Sharma et al., 2018).

Functionally, we observe that the FSS mutant myosin heavy chain proteins have abnormal ATPase kinetics (Walklate et al., 2016). The T178I mutation had the strongest reduction in MHC ATPase activity (Fig. 6B). This fits well with a genotype-phenotype correlative study in FSS patients, where it was found that the T178I mutation led to the most severe phenotypes in those patients compared to R672H and R672C mutations (Beck et al., 2014). Some reports indicate that altered muscle contractility during development lead to contractures (Bamshad et al., 2009; Robinson et al., 2007). By modeling the effect of the mutations on myosin structure, we find that the structural modifications disturb the ATP binding pocket, which is near the mutation sites, resulting in an impairment of catalytic activity (Fig. 1D). Loss of hydrophobic packing or breaking polar interactions possibly affects the structural stability of the mutant MHC proteins. From our ATPase assay results, we observed the least ATPase activity in the T178I mutation, possibly because the T178 residue lies closer to the ATP binding region, compared to R672.

We also find that expressing the FSS mutant *Mhc* leads to delayed pupal eclosion and reduced climbing capability in *Drosophila*, indicating that the structural deficits have functional consequences. The deficit in muscle function in flies expressing the FSS mutant *Mhc* could be due to the reduced ATPase activity of the mutant MHC protein, the sarcomeric structural defects, or a combination of both. It is unclear how the MHC ATPase activity and sarcomere assembly are interconnected, although some reports have started addressing this. A recent study shows that the muscle LIM protein (MLP) and cardiac myosin-binding

protein C (MyBP-C) form a complex, which modulates myosin ATPase activity, sarcomere formation and myofilament assembly (Arvanitis et al., 2017). Another study suggests that muscle contractility during development is critical for maintenance of the muscle stem cell population and myogenic differentiation (de Lima et al., 2016). Another study using muscle cells from patients with the R672C mutation found that the mutant cells exhibited decreased force production and increased duration of relaxation (Racca et al., 2015). The most direct evidence stems from work which used specific inhibitors of myosin cross bridge-cycling and contractility, which disrupts sarcomere assembly and myofibrillogenesis (Ramachandran et al., 2003).

Thus, our work suggests that the contractures seen in FSS patients could be due to reduced ATPase activity of the mutant MyHC-embryonic protein during development. Proper MyHC-embryonic ATPase activity might be required for efficient assembly of muscle contractile proteins and sarcomere formation. Additional work on the sequence of events during sarcomere formation and a time course of when MyHC-embryonic contractility is required during development should shed light on the precise mechanisms underlying FSS and other contracture syndromes.

4 Materials and methods

4.1 Fly stocks and genetic crosses

All flies were maintained on corn meal food at 18 °C under standard conditions. Wild type *Canton S* (Bl #64349), double balancer $sna^{Sco}/CyO;\ MKRS/TM6B$ (Bl #3703) and *Mef2GAL4* on 3rd chromosome (Bl #27390) (Schnorrer et al., 2010) are from Bloomington Drosophila Stock Center. Mhc^{1}/CyO flies were provided by Sanford Bernstein (O'Donnell and Bernstein, 1988). The $UAS\text{-}Mhc^{wt}$, $UAS\text{-}Mhc^{R672H}$, $UAS\text{-}Mhc^{R672C}$ and $UAS\text{-}Mhc^{T178I}$ stocks were generated as part of this study.

Mhc^{1}/CyO males were crossed to the double balancer $sna^{Sco}/CyO;\ MKRS/TM6B$ females and the progeny were crossed to each other to select $Mhc^{1}/CyO;\ MKRS/TM6B$, which was maintained as a stock. *Mef2GAL4/Mef2GAL4* on 3rd chromosome males were crossed to the double balancer $sna^{Sco}/CyO;\ MKRS/TM6B$ females and the progeny were crossed to each other to select $sna^{Sco}/CyO;\ Mef2GAL4/Mef2GAL4$, which was maintained as a stock. $Mhc^{1}/CyO;\ MKRS/TM6B$ males were crossed to $sna^{Sco}/CyO;\ Mef2GAL4/Mef2GAL4$, and the progeny were crossed to each other to select $Mhc^{1}/CyO;\ Mef2GAL4/Mef2GAL4$, which was maintained as a stock for the final matings.

The balanced $UAS\text{-}Mhc^{wt}/TM6B$, $UAS\text{-}Mhc^{R672H}/TM6B$, $UAS\text{-}Mhc^{R672C}/TM6B$ and $UAS\text{-}Mhc^{T178I}/TM6B$ transgenic stock males were each crossed to the double balancer $sna^{Sco}/CyO;\ MKRS/TM6B$ females. The progeny were crossed to each other to recover $sna^{Sco}/CyO;\ UAS\text{-}Mhc^{*}/UAS\text{-}Mhc^{*}$, where $UAS\text{-}Mhc^{*}$ represents the $UAS\text{-}Mhc^{wt}$, $UAS\text{-}Mhc^{R672H}$, $UAS\text{-}Mhc^{R672C}$ and $UAS\text{-}Mhc^{T178I}$ transgenes. Next, $sna^{Sco}/CyO;\ UAS\text{-}Mhc^{*}/UAS\text{-}Mhc^{*}$ male flies were crossed to $Mhc^{1}/CyO;\ MKRS/TM6B$ females, and the progeny were crossed to each other to select the $Mhc^{1}/CyO;\ UAS\text{-}Mhc^{*}/UAS\text{-}Mhc^{*}$ flies, which was maintained as a stock for the final matings.

The final mating was between *Mhc*^{1}*/CyO; Mef2GAL4/Mef2GAL4* females and *Mhc*^{1}*/CyO; UAS-Mhc*/UAS-Mhc** males, from where the only surviving adult progeny were *Mhc*^{1}*/CyO; Mef2GAL4/UAS-Mhc**. These flies were analyzed for sarcomeric structural and functional defects. In addition, to test the dominant effect of MHC expression, *UAS-Mhc*^{wt}*/Mef2GAL4* flies were generated in a wild type background and analyzed for sarcomeric structural defects.

4.2 Molecular cloning and transgenesis

Drosophila Mhc cDNA (RH 59876) was procured from the Drosophila Genomics Resource Center (DGRC), Indiana University, Bloomington, and used as template to generate the transgenic constructs. Mutagenesis of *Mhc* cDNA was performed by PCR directed mutagenesis in two steps, using mutagenic primers (Supplementary Table 1). Briefly, one pair of primers was used to amplify the 5′ part of the cDNA and a second pair for the 3′ part of the cDNA, with a region of overlap between the two products, incorporating the respective mutation. Now, the 5′ part of the cDNA and the 3′ part of the cDNA are mixed together and used as template for a PCR using the forward primer used for the 5′ part and reverse primer used for the 3′ part to amplify the entire *Mhc* sequence. This product was sub-cloned into the pCR 2.1-TOPO TA cloning vector (ThermoFisher Scientific Catalog# 450641), digested with *Not*I and *Kpn*I restriction enzymes, purified and ligated into the *Drosophila pUASTattB* transgenesis vector (Bischof et al., 2007). The plasmids were sequenced to validate that the mutant residues in *Mhc* have been incorporated and that no additional mutations are present.

Transgenesis was carried out at the fly facility at Bangalore Life-Science Cluster. The four constructs (*pUASTattB-Mhc*^{wt}, *pUASTattB-Mhc*^{R672H}, *pUASTattB-Mhc*^{R672C} and *pUASTattB-Mhc*^{T178I}) were independently injected into *φC31* integrase and attP 68A4 landing site carrying embryos (Bischof et al., 2007). Germline transformant transgenic lines where successful integration of the construct occurred were identified, balanced and used for crosses.

4.3 Immunofluorescence and imaging

Flies of the desired genotype were anesthetized and immediately immersed in 100% ethanol for 1 min to remove the waxy cuticle. Then, the ethanol was aspirated out and flies were washed in 1x phosphate buffered saline (PBS). For pre-fixation, the flies were immersed in 4% paraformaldehyde solution (PFA) in PBS for 5 min and then washed in PBS.

The flies were placed ventral side up on a drop of 50% glycerol on a cold glass slide. The flies were then frozen by immersing in liquid nitrogen for 1 min. The frozen flies were bisected along the mid-ventral line to expose the thoracic halves and the DLMs. Each thoracic half was fixed in 4% PFA for 20 min, washed in 0.5% PBS with Triton-X 100 (PBSTx) for 10 min each, six times. After washing, the muscles were blocked using 1% BSA in PBSTx. Thoraces were incubated in anti-Kettin (Abcam MAC 147) primary antibody at a dilution of 1:200 overnight at 4 °C. Thoraces were then washed six times, 10 min each in PBSTx. Cy3 conjugated secondary antibody against rat Fc (112-165-167, Jackson Immunoresearch) and Oregon 488 Phalloidin (Thermo Scientific Cat # 07466) were

Europe PMC Funders Author Manuscripts

added at a dilution of 1:500 in blocking solution and incubated at room temperature for 2 h. Thoraces were then washed six times, 10 min each in PBSTx and mounted in Vectashield with DAPI (Vector laboratories Catalog No. H-1200) and coverslips were sealed at the edges with clear nail paint. Immunofluorescence images were acquired using a Leica SP8 confocal microscope.

4.4 Sarcomere and fiber measurements

Exported image files were quantified using the LAS X application suite for inter Z-disc length and Z-disc width measurements. Using line function, a region of interest (ROI) was drawn parallel to the muscle fiber spanning 6 sarcomeres in a single Z-stack. Inter Z-disc length (um) was measured as the distance between two consecutive Z-discs, measuring from the mid-point of Z-disc intensity (Cammarato et al., 2011). A minimum of 5 sarcomeres per muscle fiber for 4–5 fibers were quantified from 9 images using 5 different replicates for each genotype at 5 and 20 days of age (*Canton S*, Mhc^{1}/CyO; $Mef2GAL4/UAS\text{-}Mhc^{wt}$, Mhc^{1}/CyO; $Mef2GAL4/UAS\text{-}Mhc^{R672H}$, Mhc^{1}/CyO; $Mef2GAL4/UAS\text{-}Mhc^{R672C}$ and Mhc^{1}/CyO; $Mef2GAL4/UAS\text{-}Mhc^{T178I}$).

For Z-disc width, the scale bar function was used for measurement. A scaled line was drawn parallel to the Z-disc and the width was quantified in um. Similar to sarcomere size quantification, a minimum of 5 sarcomeres per muscle fiber for 4–5 fibers were quantified from 9 images using 5 different replicates for each genotype (*Canton S*, Mhc^{1}/CyO; $Mef2\text{-}GAL4/UAS\text{-}Mhc^{wt}$, Mhc^{1}/CyO; $Mef2GAL4/UAS\text{-}Mhc^{R672H}$, Mhc^{1}/CyO; $Mef2GAL4/UAS\text{-}Mhc^{R672C}$ and Mhc^{1}/CyO; $Mef2GAL4/UAS\text{-}Mhc^{T178I}$), both at 5 and 20 days of age.

For fiber splitting analysis, the number of split fibers and the total number of fibers were counted by the count tool in Adobe Photoshop CS6. At least 3 images were used per genotype, and a minimum of 20 fibers were counted per image. The ratio of split fiber number to the total fiber number in the image was used to calculate the percentage of fiber splitting.

4.5 Pupal eclosion assay

Pupae within 1 h of puparium formation from uncrowded vials were collected gently with a soft, wet paintbrush and transferred to a petri dish with moist blotting paper. The petri dishes were labeled for the genotype, date and hour of collection and pupae allowed to mature at 25 °C. The pupae were observed for eclosion every few hours. The time of eclosion of each fly was noted and the number of hours taken by each fly to complete the pupal stage was calculated.

4.6 Climbing assay

Approximately 15–20 flies were anesthetized and transferred to a 15 ml plastic centrifuge tube and allowed to recover from anesthesia for 30 min. After recovery, flies were tapped to bring them to the bottom of the tube and allowed to climb while being video recorded. Climbing index was calculated as the percentage of flies that crossed the 8 cm mark, were in the 4–8 cm range, or below 4 cm mark on the tube in 10 s modified from (Ali et al., 2011). Readings were taken a minimum of 3 times using at least 2 sets of 15 or more flies.

4.7 Actin and myosin isolation and ATPase assay

Actin was isolated from mouse skeletal muscle (Racusen and Thompson, 1996). Myosin Heavy Chain (MHC) protein was isolated from the dorsal longitudinal muscles (DLMs) of ~50 flies. Flies were anesthetized and immersed in absolute ethanol for 1 min to remove the cuticle. To isolate DLMs, flies were dissected on a cold glass slide in York's Modified Glycerol (YMG) (20 mM Potassium Phosphate, pH 7.0, 2 mM $MgCl_2$, 1 mM EGTA, 8 mM DTT, 50% (v/v) glycerol and 1x protease inhibitor cocktail) and stored in YMG at 0 °C until all the samples were dissected (Swank et al., 2001). The DLMs were centrifuged at 2 °C, 8500x*g* for 10 min to make them settle, YMG was replaced with YMGT (20 mM Potassium Phosphate, pH 7.0, 2 mM $MgCl_2$, 1 mM EGTA, 8 mM DTT, 2% v/v Triton X-100 and 1x protease inhibitor cocktail) and the mixture was incubated on ice for 30 min. After 30 min, DLMs were washed thrice in YMG without glycerol (20 mM Potassium Phosphate, pH 7.0, 2 mM $MgCl_2$, 1 mM EGTA, 8 mM DTT, 1x protease inhibitor cocktail). Myosin was extracted in 50 µL of Myosin Extraction Buffer (1.0 M KCl, 0.15 M potassium phosphate, pH 6.8, 10 mM sodium pyro-phosphate, 5 mM $MgCl_2$, 0.5 mM EGTA, 8 mM DTT and 1x protease inhibitor cocktail). The myosin was loaded onto a 100 kDa cut-off column and washed thrice in Myosin Storage buffer (MSB) (0.5 M KCl, 20 mM MOPS, pH 7.0, 2 mM $MgCl_2$ and 8 mM DTT) with 5 mM ATP and thrice in MSB without ATP. The final retentate was aliquoted and stored on ice for protein estimation (CB-X protein estimation kit, G Biosciences, Cat# 786-11X) and ATP hydrolysis assay.

ATPase assay was carried out using the EnzCheck Phosphate Assay Kit (E6646 ThermoFisher Scientific). Briefly, ATPase assay was done by adding 10 µg of MHC to a standard reaction mix of 100 µl of MESG (2-amino-6-marcapto-7-methyl-purine riboside), 5 µl PNP (purine nucleoside phosphorylase), 25 µl of 20x reaction buffer (1M Tris-HCl, 20 mM $MgCl_2$, pH 7.5 and 2 mM sodium azide) and Actin to a final concentration of 2 µM. The reaction volume was made up to 500 µl with water and incubated at room temperature for 10 min to eliminate any free phosphate in the reaction mixture. The mixture was transferred to a quartz cuvette and reaction was started by adding ATP to a final concentration 400 µM. The absorbance was measured at 360 nm at intervals of 6 s for 1 h.

A no-actin control ATPase assay was carried out without the addition of Actin. All components of the ATPase assay were added at the same concentration except for Actin and absorbance was read for 1 h at 360 nm at intervals of 6 s.

4.8 Statistical analysis

Data was analyzed using parametric, unpaired *t*-test and one-way Anova (pupal eclosion and fiber splitting) using GraphPad prism software. Graphs are presented as Mean ± standard error of the mean. The p-values are indicated on the graphs and p-value ≤ 0.05 are considered significant, marked by asterisks.

Supplementary Material

Refer to Web version on PubMed Central for supplementary material.

Acknowledgements

We thank Prof. K. VijayRaghavan (NCBS, Bangalore) and his lab members for providing training on fly muscle preparations. We are grateful to Prof. Sanford Bernstein (SDSU, California) for providing some of the *Drosophila* stocks used in this study. The transgenic fly lines were generated on payment basis at the fly facility at Bangalore LifeScience Cluster. We acknowledge the imaging and central instrumentation facilities at RCB. We thank Dr. Deepti Jain (RCB, Faridabad) and her lab members for help with the ATPase assay. Authors acknowledge the support of DBT e-Library Consortium (DeLCON) for providing access to e-resources. Stocks obtained from the Bloomington Drosophila Stock Center (NIH P40OD018537) were used in this study. We acknowledge critical comments and suggestions from all members of the Developmental Genetics Laboratory, RCB.

Funding

This work was supported by the Wellcome Trust/DBT India Alliance through an intermediate fellowship (IA/I/13/1/500872) to SJM. We also acknowledge core funds provided by the Regional Centre for Biotechnology (RCB). PK is funded by a Council for Scientific and Industrial Research (CSIR) senior research fellowship.

References

Ali YO, Escala W, Ruan K, Zhai RG. Assaying locomotor, learning, and memory deficits in Drosophila models of neurodegeneration. J Visualized Exp JoVE. 2011; (49):2504.

Arvanitis DA, Vafiadaki E, Papalouka V, Sanoudou D. Muscle Lim Protein and myosin binding protein C form a complex regulating muscle differentiation. Biochim Biophys Acta (BBA) Mol Cell Res. 2017; 1864:2308–2321.

Bai J, Hartwig JH, Perrimon N. SALS, a WH2-domain-containing protein, promotes sarcomeric actin filament elongation from pointed ends during Drosophila muscle growth. Dev Cell. 2007; 13:828–842. [PubMed: 18061565]

Bamshad M, Van Heest AE, Pleasure D. Arthrogryposis: a review and update. J Bone Joint Surg Am. 2009; 91:40.

Beck AE, McMillin MJ, Gildersleeve HI, Shively KM, Tang A, Bamshad MJ. Genotype-phenotype relationships in Freeman–Sheldon syndrome. Am J Med Genet Part A. 2014; 164:2808–2813.

Bischof J, Maeda RK, Hediger M, Karch F, Basler K. An optimized transgenesis system for Drosophila using germ-line-specific φC31 integrases. Proc Natl Acad Sci. 2007; 104:3312–3317. [PubMed: 17360644]

Cammarato A, Li XE, Reedy MC, Lee CF, Lehman W, Bernstein SI. Structural basis for myopathic defects engendered by alterations in the myosin rod. J Mol Biol. 2011; 414:477–484. [PubMed: 22037585]

de Lima JE, Bonnin M-A, Birchmeier C, Duprez D. Muscle contraction is required to maintain the pool of muscle progenitors via YAP and NOTCH during fetal myogenesis. Elife. 2016; 5:e15593. [PubMed: 27554485]

Dougherty DA. Cation-pi interactions in chemistry and biology: a new view of benzene, Phe, Tyr, and Trp. Science. 1996; 271:163–168. [PubMed: 8539615]

Gunage RD, Reichert H, VijayRaghavan K. Identification of a new stem cell population that generates Drosophila flight muscles. Elife. 2014; 3:e03126.

Hatfield I, Harvey I, Yates ER, Redd JR, Reiter LT, Bridges D. The role of TORC1 in muscle development in Drosophila. Sci Rep. 2015; 5

Kimber E, Tajsharghi H, Kroksmark AK, Oldfors A, Tulinius M. Distal arthrogryposis: clinical and genetic findings. Acta Paediatr. 2012; 101:877–887. [PubMed: 22519952]

O'Donnell PT, Bernstein SI. Molecular and ultrastructural defects in a Drosophila myosin heavy chain mutant: differential effects on muscle function produced by similar thick filament abnormalities. J Cell Biol. 1988; 107:2601–2612. [PubMed: 2462566]

Racca AW, Beck AE, McMillin MJ, Korte FS, Bamshad MJ, Regnier M. The embryonic myosin R672C mutation that underlies Freeman-Sheldon syndrome impairs cross-bridge detachment and cycling in adult skeletal muscle. Hum Mol Genet. 2015; 24:3348–3358. [PubMed: 25740846]

Racusen, RH; Thompson, KV. Isolation of myosin and actin from chicken muscle. Proceedings of the 18th Workshop/Conference of the Association for Biology Laboratory Education (ABLE); 1996. 97–111.

Ramachandran I, Terry M, Ferrari MB. Skeletal muscle myosin cross-bridge cycling is necessary for myofibrillogenesis. Cell Motil Cytoskelet. 2003; 55:61–72.

Robinson P, Lipscomb S, Preston LC, Altin E, Watkins H, Ashley CC, Redwood CS. Mutations in fast skeletal troponin I, troponin T, and β-tropomyosin that cause distal arthrogryposis all increase contractile function. FASEB J. 2007; 21:896–905. [PubMed: 17194691]

Rui Y, Bai J, Perrimon N. Sarcomere formation occurs by the assembly of multiple latent protein complexes. PLoS Genet. 2010; 6:e1001208. [PubMed: 21124995]

Schiaffino S, Reggiani C. Molecular diversity of myofibrillar proteins: gene regulation and functional significance. Physiol Rev. 1996; 76:371–423. [PubMed: 8618961]

Schnorrer F, Schönbauer C, Langer CC, Dietzl G, Novatchkova M, Schernhuber K, Fellner M, Azaryan A, Radolf M, Stark A. Systematic genetic analysis of muscle morphogenesis and function in Drosophila. Nature. 2010; 464:287. [PubMed: 20220848]

Sellers JR. Myosins: a diverse superfamily. Biochim Biophys Acta (BBA) Mol Cell Res. 2000; 1496:3–22.

Sharma A, Agarwal M, Kumar A, Kumar P, Saini M, Kardon G, Mathew S. Myosin heavy chain-embryonic is a crucial regulator of skeletal muscle development and differentiation. bioRxiv. 2018; doi: 10.1101/261685

Swank DM, Bartoo ML, Knowles AF, Iliffe C, Bernstein SI, Molloy JE, Sparrow JC. Alternative exon-encoded regions of Drosophila myosin heavy chain modulate ATPase rates and actin sliding velocity. J Biol Chem. 2001; 276:15117–15124. [PubMed: 11134017]

Tajsharghi H, Kimber E, Kroksmark AK, Jerre R, Tulinius M, Oldfors A. Embryonic myosin heavy-chain mutations cause distal arthrogryposis and developmental myosin myopathy that persists postnatally. Arch Neurol. 2008; 65:1083–1090. [PubMed: 18695058]

Toydemir RM, Rutherford A, Whitby FG, Jorde LB, Carey JC, Bamshad MJ. Mutations in embryonic myosin heavy chain (MYH3) cause Freeman-Sheldon syndrome and Sheldon-Hall syndrome. Nat Genet. 2006; 38:561. [PubMed: 16642020]

Walklate J, Vera C, Bloemink MJ, Geeves MA, Leinwand L. The most prevalent Freeman-Sheldon syndrome mutations in the embryonic myosin motor share functional defects. J Biol Chem. 2016; 291(19):10318–10331. [PubMed: 26945064]

Webb MR. A continuous spectrophotometric assay for inorganic phosphate and for measuring phosphate release kinetics in biological systems. Proc Natl Acad Sci. 1992; 89:4884–4887. [PubMed: 1534409]

Wheeler SE, Bloom JW. Toward a more complete understanding of noncovalent interactions involving aromatic rings. J Phys Chem A. 2014; 118:6133–6147. [PubMed: 24937084]

Europe PMC Funders Author Manuscripts

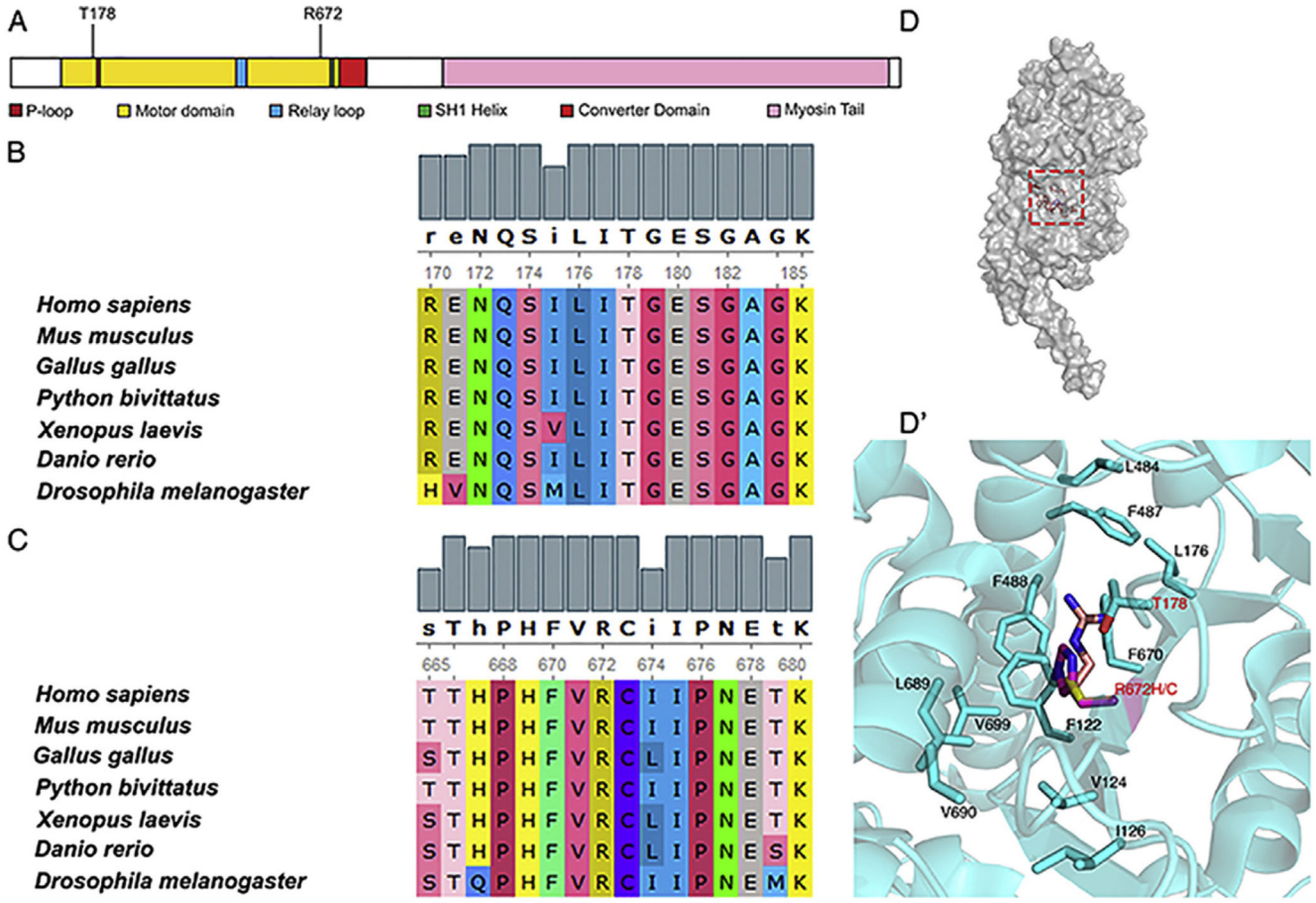

Fig. 1. The T178 and R672 residues in MyHC-embryonic which are mutated in FSS are evolutionarily conserved.

MyHC-embryonic protein schematic with the major protein domains and motifs labeled, showing the position of the T178 and R672 residues, which are the most frequently mutated residues in FSS (A). The T178 and R672 residues from human MyHC-embryonic were aligned to myosin heavy chain proteins from different vertebrate classes and the *Drosophila* myosin heavy chain using ClustalW (B, C). Both residues and neighboring residues are conserved across evolution (B, C). Surface representation of the monomer unit of *Drosophila* MHC (D). Magnified view of the boxed region in D showing the residues which are involved in hydrophobic packing in the ATP binding site of MHC (D′). Panel D and D′ are drawn in Pymol version 1.8 (PDB ID 5W1A). The R672 residue is mutated to H or C (R is light pink, C is yellow, and H is magenta).

Europe PMC Funders Author Manuscripts

Europe PMC Funders Author Manuscripts

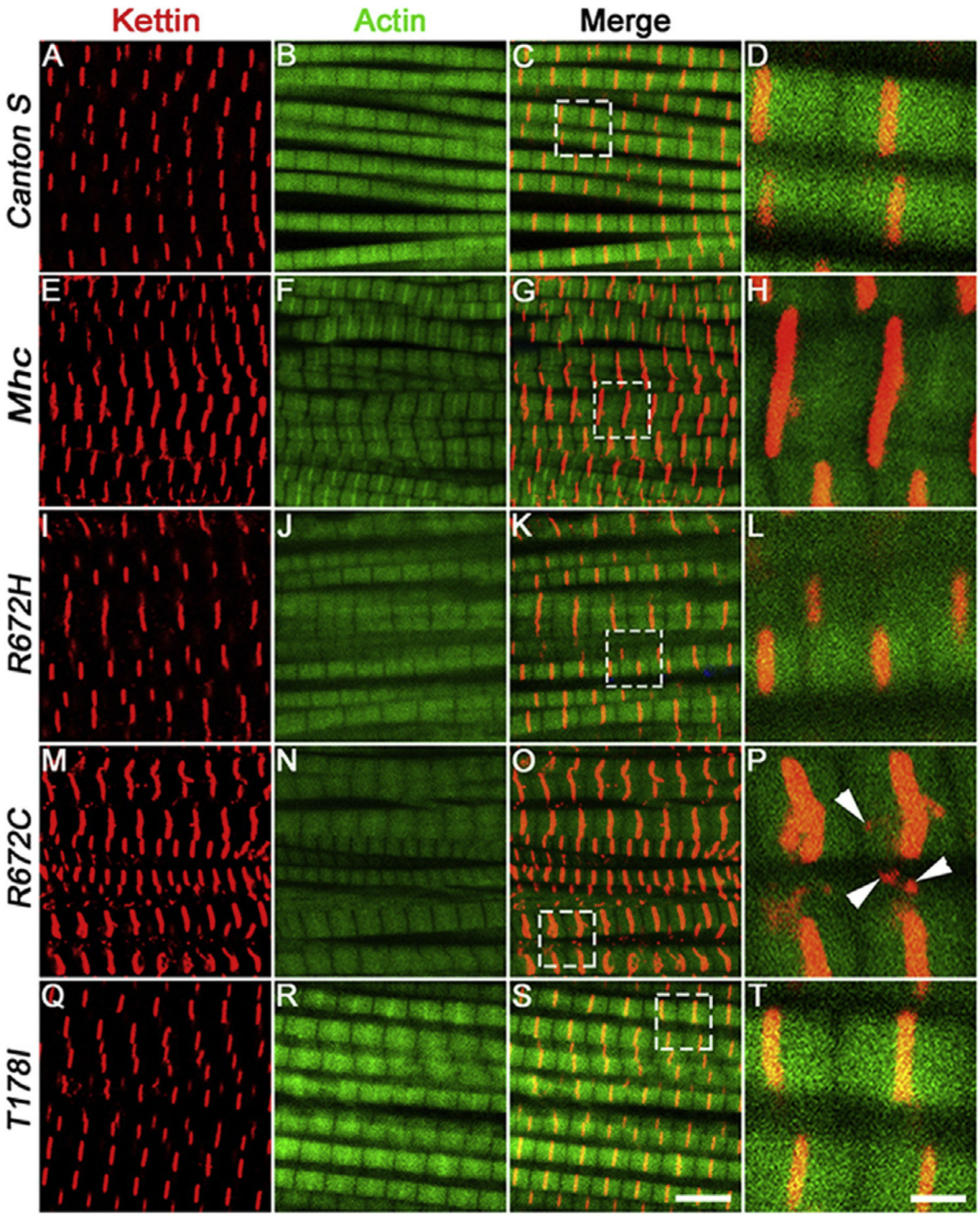

Fig. 2. Expression of FSS mutant *Mhc* transgenes lead to fiber branching and Z-disc defects 5 days post-eclosion.

Representative dorsal longitudinal muscles (DLMs) from wild type *Canton S* (A–D), *Mhc^{1}/CyO; Mef2GAL4/UAS-Mhc^{wt}* (E–H), *Mhc^{1}/CyO; Mef2GAL4/UAS-Mhc^{R672H}* (I–L), *Mhc^{1}/CyO; Mef2-GAL4/UAS-Mhc^{R672C}* (M–P) *and Mhc^{1}/CyO; Mef2GAL4/UAS-Mhc^{T178I}* (Q–T), 5 days post-eclosion, labeled by immunofluorescence for Kettin marking the Z-disc (red), and Actin labeling the thin filament (green). The boxed regions in the merge images C, G, K, O and S are magnified and shown in D, H, L, P and T respectively. Arrowheads in P point to Kettin puncta that are not part of the Z-disc. All images are from a

single, representative Z-plane from one of the replicates. Scale bar in S is 5 μm and T is 1 μm.

Europe PMC Funders Author Manuscripts

Europe PMC Funders Author Manuscripts

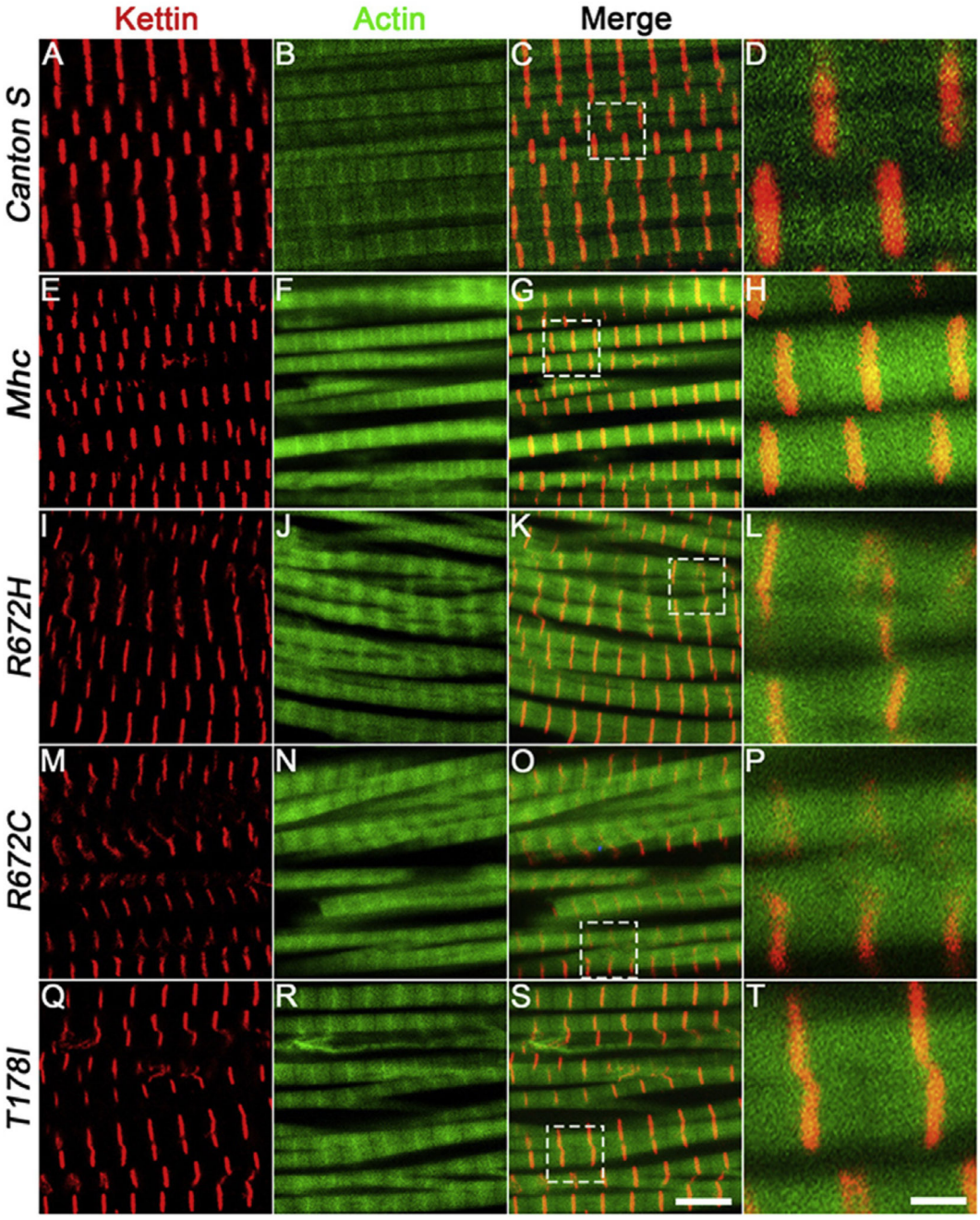

Fig. 3. Expression of FSS mutant *Mhc* transgenes lead to fiber branching and Z-disc defects 20 days post-eclosion.

Representative dorsal longitudinal muscles (DLMs) from wild type *Canton S* (A–D), *Mhc^{1}/CyO; Mef2GAL4/UAS-Mhc^{wt}* (E–H), *Mhc^{1}/CyO; Mef2GAL4/UAS-Mhc^{R672H}* (I–L), *Mhc^{1}/CyO; Mef2-GAL4/UAS-Mhc^{R672C}* (M–P) *and Mhc^{1}/CyO; Mef2GAL4/UAS-Mhc^{T178I}* (Q–T), 20 days post-eclosion, labeled by immunofluorescence for Kettin marking the Z-disc (red), and Actin labeling the thin filament (green). The boxed regions in the merge images C, G, K, O and S are magnified and shown in D, H, L, P and T respectively.

All images are from a single, representative Z-plane from one of the replicates. Scale bar in S is 5 μm and T is 1 μm.

Europe PMC Funders Author Manuscripts

Europe PMC Funders Author Manuscripts

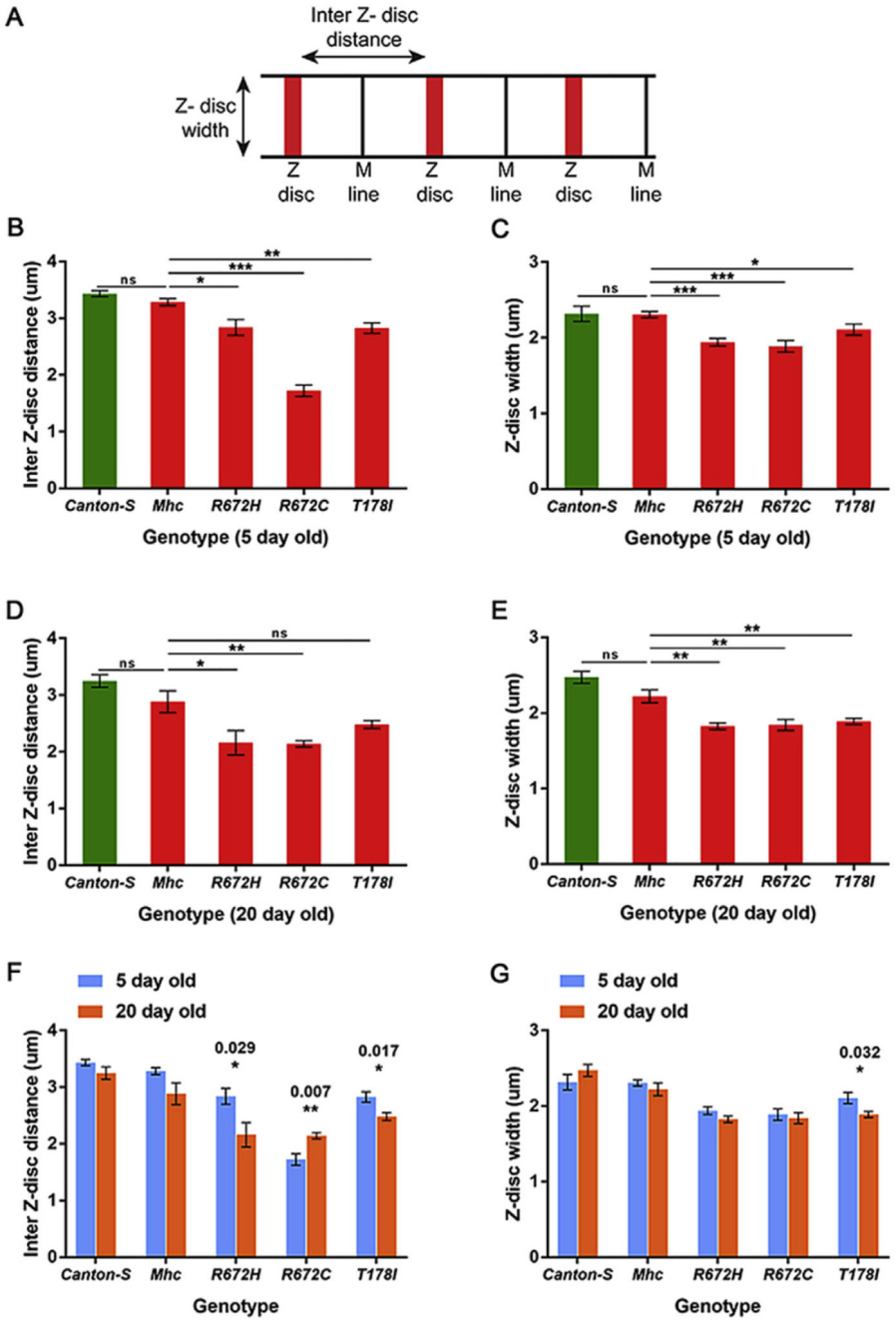

Fig. 4. Inter Z-disc distance and Z-disc width are significantly reduced in sarcomeres of flies expressing the FSS mutant *Mhc* transgenes.

Schematic of a myofiber, depicting the inter Z-disc distance and Z-disc width (A). Quantification of the inter Z-disc distance 5 (B) and 20 (D) days post-eclosion, and Z-disc width 5 (C) and 20 (E) days post-eclosion respectively in DLMs of wild type *Canton S*, Mhc^{1}/CyO; $Mef2GAL4/UAS\text{-}Mhc^{wt}$, Mhc^{1}/CyO; $Mef2GAL4/UAS\text{-}Mhc^{R672H}$, Mhc^{1}/CyO; $Mef2GAL4/UAS\text{-}Mhc^{R672C}$ and Mhc^{1}/CyO; $Mef2GAL4/UAS\text{-}Mhc^{T178I}$ flies. The inter Z-disc distance (F) and Z-disc width (G) at 5 days post-eclosion compared to 20 days post-

eclosion for each genotype. The graphical data is presented as mean ± standard error of the mean using a minimum of 5 replicates.

Europe PMC Funders Author Manuscripts

Europe PMC Funders Author Manuscripts

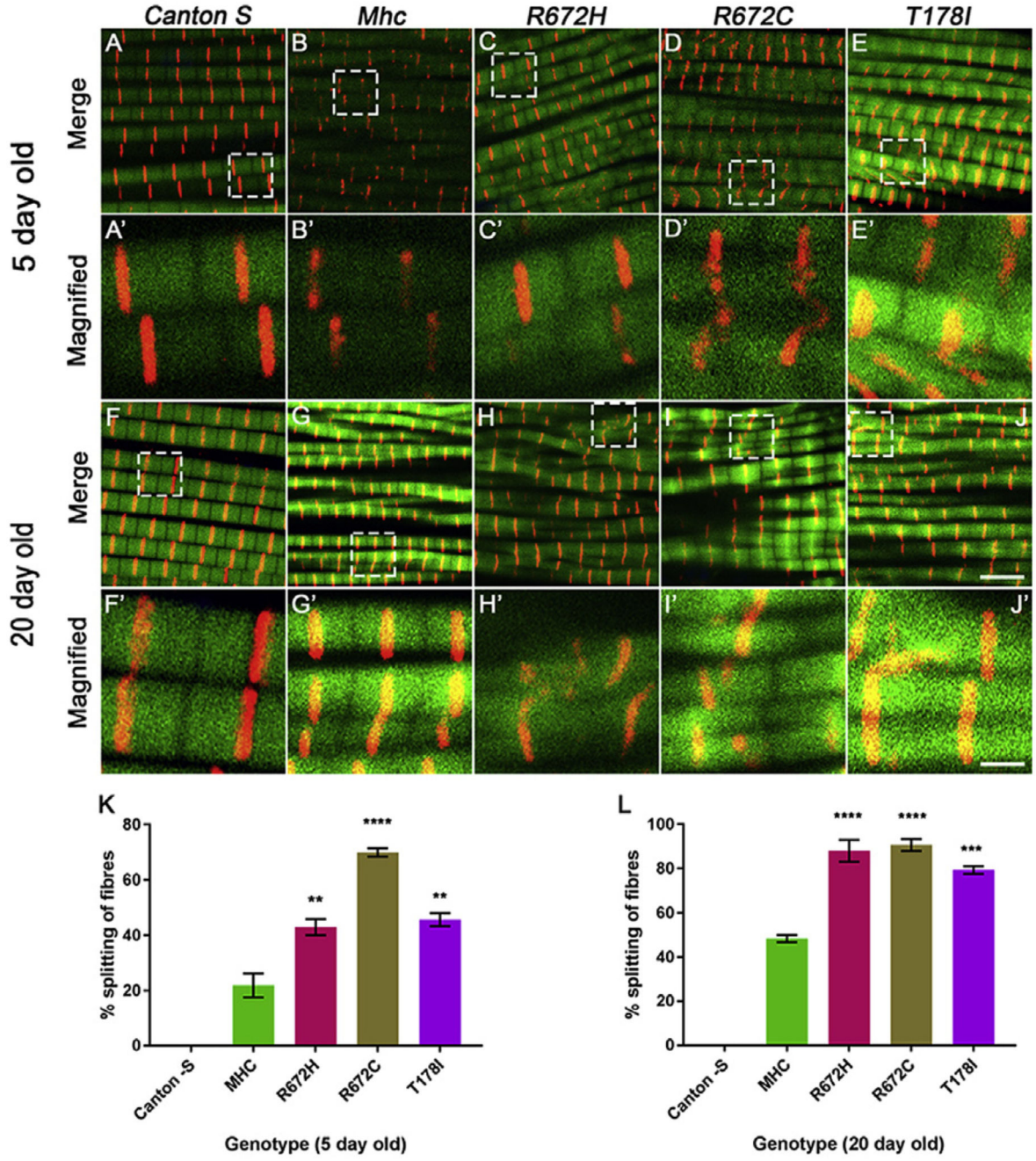

Fig. 5. Expression of FSS mutant *Mhc* transgenes lead to increased fiber splitting 5 and 20 days post-eclosion.

Representative dorsal longitudinal muscles (DLMs) from 5 to 20 days post-eclosion wild type *Canton S* (A-A′, F-F′), *Mhc*^{1}*/CyO; Mef2GAL4/UAS-Mhc*^{wt} (B-B′, G-G′), *Mhc*^{1}*/CyO; Mef2GAL4/UAS-Mhc*^{R672H} (C-C′, H-H′), *Mhc*^{1}*/CyO; Mef2GAL4/UAS-Mhc*^{R672C} (D-D′, I-I′) *and Mhc*^{1}*/CyO; Mef2GAL4/UAS-Mhc*^{T178I} (E-E′, J-J′), labeled by immunofluorescence for Kettin marking the Z-disc (red), and Actin labeling the thin filament (green). A-E′ are DLMs from 5 days post-eclosion flies and F-J′ are DLMs from 20 days post-eclosion flies. The boxed regions in the images A-E and F-J are magnified and

shown in A′-E′ and F′-J′ respectively. Quantification of the percentage of split fibers as a proportion of total fibers for DLMs from each genotype at 5 days (K) and 20 days (L) post-eclosion are shown. The graphical data is presented as mean ± standard error of the mean using a minimum of 5 replicates. Scale bar in J is 5 μm and J′ is 1 μm.

Europe PMC Funders Author Manuscripts

Europe PMC Funders Author Manuscripts

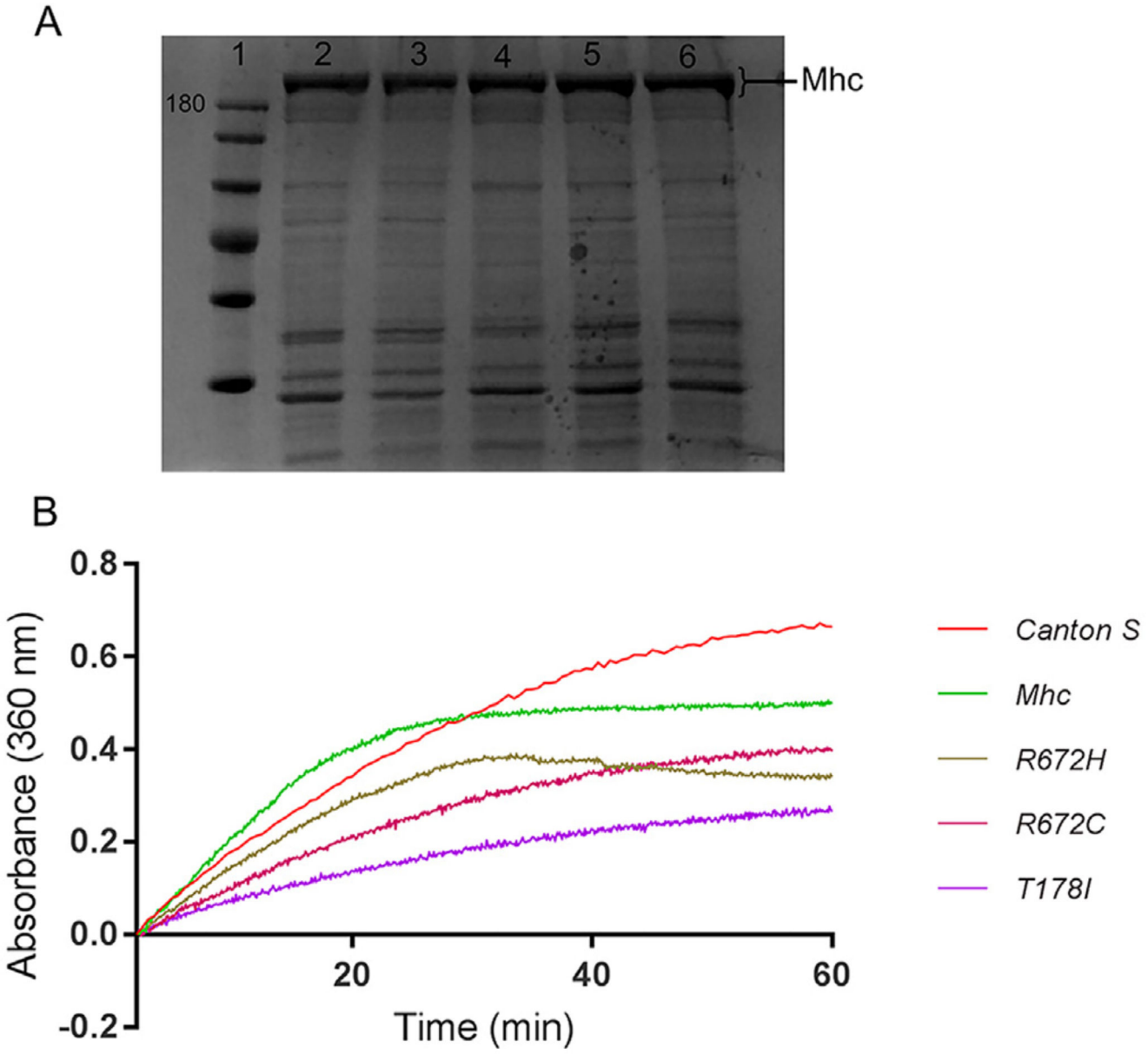

Fig. 6. FSS mutant MHC exhibit decreased ATPase activity.

Coomassie stained SDS-PAGE showing MHC protein (high molecular weight band of about 205 KDa), where lane 1 is molecular weight marker with 180 KDa band labeled, and lanes 2–6 are protein samples enriched for MHC (2 μg each) from DLMs of wild type *Canton S* (lane 2), *Mhc^{1}/CyO; Mef2GAL4/UAS-Mhc^{wt}* (lane 3), *Mhc^{1}/CyO; Mef2GAL4/UAS-Mhc^{T178I}* (lane 4), *Mhc^{1}/CyO; Mef2GAL4/UAS-Mhc^{R672H}* (lane 5) *and Mhc^{1}/CyO; Mef2GAL4/UAS-Mhc^{R672C}* (lane 6) flies respectively (A). Rate of phosphate released by the MHC ATPase indicated by absorbance at 360 nm as a function of time (B). The graphs are normalized to a reaction mix without ATP. Graphs indicate that the ATPase activity is reduced in the 3 FSS mutant *Mhc* transgenic lines compared to controls, with the most

drastic reduction observed in the case of T178I mutation (B). Data shown here is from a single assay.

Europe PMC Funders Author Manuscripts

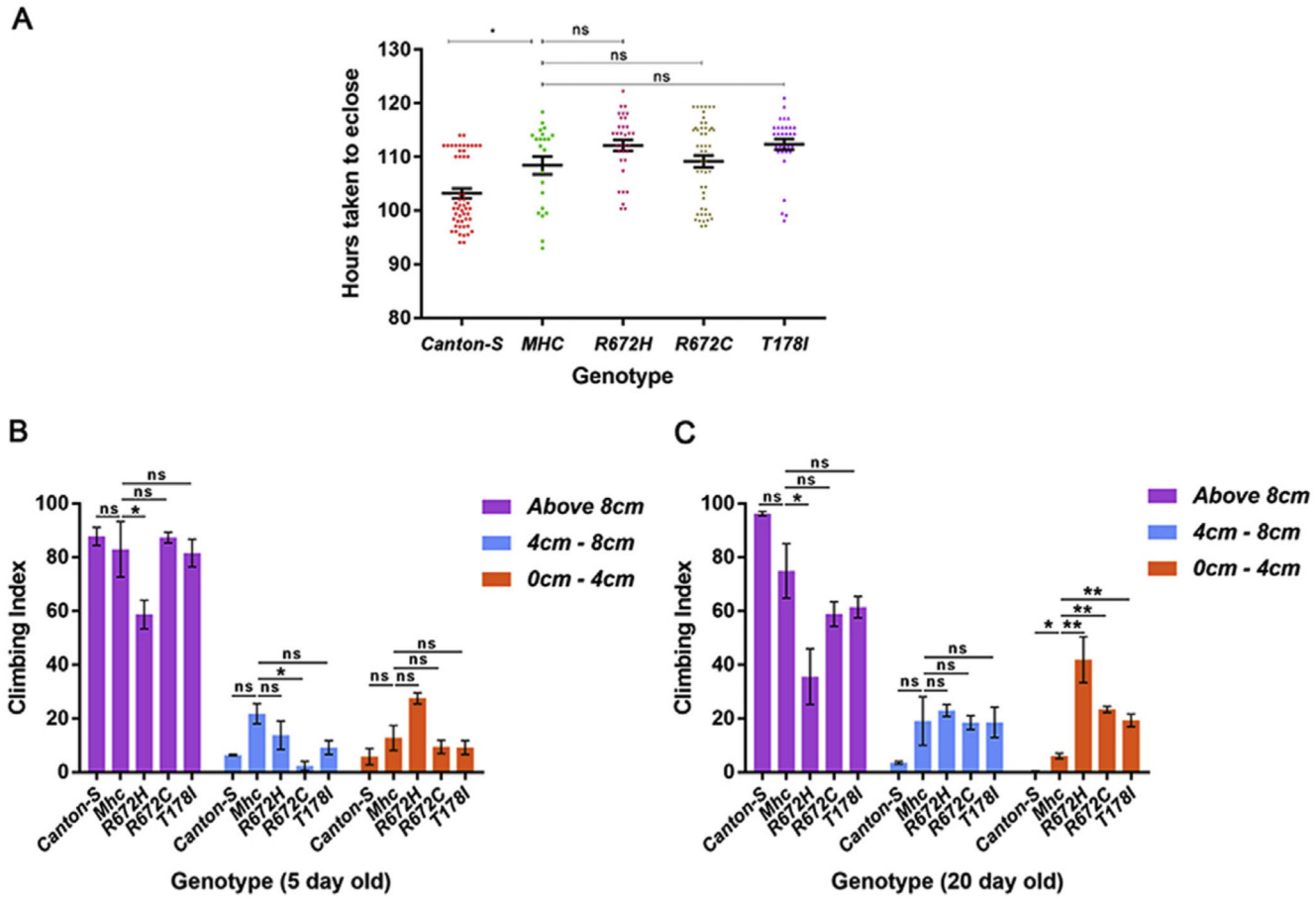

Fig. 7. Expression of FSS mutant *Mhc* transgenes lead to defects in muscle function.

The pupal duration was quantified in wild type *Canton S*, Mhc^{1}*/CyO; Mef2GAL4/UAS-*Mhc^{wt}, Mhc^{1}*/CyO; Mef2GAL4/UAS-*Mhc^{R672H}, Mhc^{1}*/CyO; Mef2GAL4/UAS-*Mhc^{R672C} *and* Mhc^{1}*/CyO; Mef2GAL4/UAS-*Mhc^{T178I} flies (A). Climbing assay to test muscle function was carried out at 5 (B) and 20 (C) days post-eclosion using wild type *Canton S*, Mhc^{1}*/CyO; Mef2GAL4/UAS-*Mhc^{wt}, Mhc^{1}*/CyO; Mef2GAL4/UAS-*Mhc^{R672H}, Mhc^{1}*/CyO; Mef2-GAL4/UAS-*Mhc^{R672C} *and* Mhc^{1}*/CyO; Mef2GAL4/UAS-*Mhc^{T178I} flies respectively. Number of flies that climbed 8 cm or above, 4–8 cm or 0–4 cm were counted, and the percentage of each category is represented as the climbing index. The graphical data is presented as mean ± standard error of the mean.

Europe PMC Funders Author Manuscripts